Deep-Sea Research Part II 147 (2018) 116–126

Contents lists available at ScienceDirect

Deep-Sea Research Part II

journal homepage: www.elsevier.com/locate/dsr2

Spatial and temporal variation in winter condition of juvenile Pacific herring (*Clupea pallasii*) in Prince William Sound, Alaska: Oceanographic exchange with the Gulf of Alaska

Kristen B. Gorman[a,*], Thomas C. Kline Jr[a], Megan E. Roberts[a], Fletcher F. Sewall[b], Ron A. Heintz[b], W. Scott Pegau[a]

[a] Prince William Sound Science Center, 300 Breakwater Ave., PO Box 705, Cordova, AK 99574, United States
[b] NOAA Alaska Fisheries Science Center, Auke Bay Laboratories, Ted Stevens Marine Research Institute, 17109 Pt. Lena Loop Road, Juneau, AK 99801, United States

ARTICLE INFO

Keywords:
Clupea pallasii
Energetics
Gulf of Alaska
Oceanographic exchange
Overwinter
Pacific herring
Prince William Sound
Stable isotope

ABSTRACT

Spatial variability in early and late winter measures of whole body energy density of juvenile (age-0) Pacific herring (*Clupea pallasii*) of Prince William Sound (PWS), Alaska was examined over nine years of study. Pacific herring in this region remain considered as an injured resource over the 25 years following the *Exxon Valdez* oil spill, however factors responsible for the lack of recovery by herring in PWS are a source of ongoing debate. Given the species' key ecological role in energy transfer to higher predators, and its economic role in a historical commercial fishery within the region, significant research effort has focused on understanding environmental factors that shape nutritional processes and the quality of these young forage fish. During November (early winter), factors such as juvenile herring body size, hydrological region of PWS, year, and the interaction between carbon ($\delta^{13}C'$) or nitrogen ($\delta^{15}N$) stable isotope signature and hydrological region were all important predictors of juvenile herring energy density. In particular, analyses indicated that in the northern and western regions of PWS, juvenile herring with more depleted $\delta^{13}C'$ values (which reflect a Gulf of Alaska carbon source) were more energy dense. Results suggest that intrusion of water derived from the Gulf of Alaska enhances the condition of age-0 herring possibly through alterations in zooplankton community structure and abundance, particularly in the northern and western regions of PWS in the fall, which is consistent with regional circulation. During March (late winter), factors such as juvenile herring body size, year, and the interaction between $\delta^{13}C'$ or $\delta^{15}N$ isotope signature and year were all important predictors of juvenile herring energy density. Results differed for early and late winter regarding the interaction between stable isotope signatures and region or year, suggesting important seasonal aspects of circulation contribute to variation in PWS juvenile herring energy density. In addition, winter-feeding may enrich herring without considerable energy gain, removing any relationship between energy density and $\delta^{13}C'$ isotope signature in late winter.

1. Introduction

Important oceanographic exchange has been described between the Gulf of Alaska (GoA) and Prince William Sound (PWS), a complex fjord-estuary located at the GoA's northernmost boundary (Fig. 1). For example, Kline (1997, 1999a, 1999b, 2001, 2009) relied on naturally occurring ratios of stable carbon ($^{13}C/^{12}C$, $\delta^{13}C$) and nitrogen ($^{15}N/^{14}N$, $\delta^{15}N$) isotope signatures of zooplankton and forage fishes to demonstrate isotopic gradients between the GoA and PWS, and subsequent oceanographic exchange between the regions driven by circulation. A strong gradient in $\delta^{13}C$ was confirmed as *Neocalanus cristatus* copepods collected from the GoA were depleted in $\delta^{13}C$ relative to those collected from within PWS, which contrasts with a weak gradient based on $\delta^{15}N$ of *N. cristatus* (Kline, 2009). Stable isotope techniques are a particularly robust method for discerning oceanographic exchange as the ratio of heavy to light isotopes of carbon and nitrogen in tissues can provide both *source* and *process* information due to isotopic fractionation (Peterson and Fry, 1987). For example, variation in the fractionation of carbon during photosynthesis can distinguish sources of primary productivity such as between nearshore and pelagic phytoplankton (Kelly, 2000). Thus, $\delta^{13}C$ values provide *source* information due to the origins of the carbon signature and the fact that $\delta^{13}C$ tends not to vary greatly across trophic levels (Peterson and Fry, 1987). However, $\delta^{15}N$ values capture a distinct signature of trophic position due to the differential

* Corresponding author.
E-mail address: kgorman@pwssc.org (K.B. Gorman).

http://dx.doi.org/10.1016/j.dsr2.2017.10.010

Available online 12 October 2017

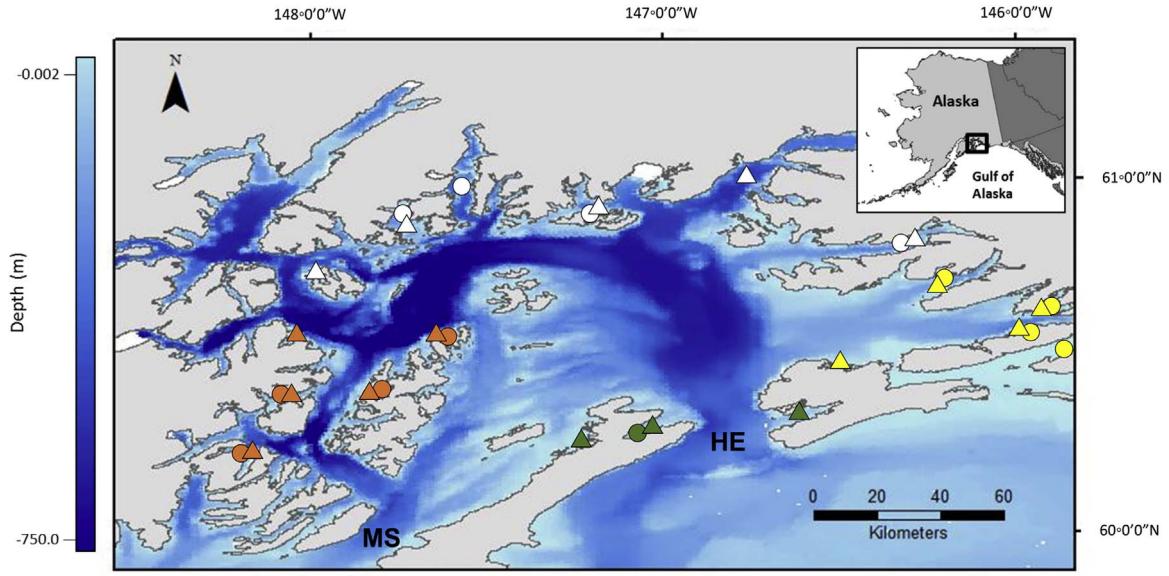

Fig. 1. Bathymetry and location of Prince William Sound nursery bays sampled for juvenile Pacific herring. Bathymetry is noted by the blue gradient, November sampling locations are noted by circles, and March sampling locations are noted by triangles. Hydrological regions included Central (green), North (white), West (orange), and East (yellow). Hinchinbrook Entrance and Montague Strait are noted as HE and MS, respectively.

excretion of the lighter isotope by consumers (Peterson and Fry, 1987). Thus, as elements such as carbon and nitrogen are produced and consumed throughout a food-web, they fractionate and are reflected in plant and animal tissues at varying time scales due to isotopic turnover rates related to metabolic activity, and for these reasons provide excellent information on the origin and distribution, or trophic position, of consumers (Deniro and Epstein, 1978, 1981).

Oceanographic exchange between the GoA and PWS, and relationships between general circulation and trophic linkages among PWS biota became increasingly important topics following the grounding of the *Exxon Valdez* oil tanker on Bligh Reef in March 1989, which reportedly released ~11 million gallons of crude oil into the coastal marine environment damaging apex predators, fish populations and other species, as well as valuable commercial fisheries such as Pink Salmon (*Onchorynchus gorbuscha*) and Pacific Herring (*Clupea pallasii*, hereafter herring) (Brown et al., 1996; Cooney et al., 2001a; Norcross et al., 2001). Factors responsible for the ongoing lack of recovery by herring in Prince William Sound are a source of ongoing debate (Ward et al., 2017). Early studies following the spill, as part of the Sound Ecosystem Assessment (SEA) program, took an integrated ecosystem approach to better understand how environmental factors might additionally be influencing the recovery of injured populations (Cooney et al., 2001a). The SEA program outlined key hypotheses that have continued to shape current research and particularly the work described here. In the context of the current study, the SEA program's "river-lake" hypothesis provides a framework for testing ideas regarding trophic linkages between the GoA and PWS that are driven by seasonal circulation. The "river-lake" hypothesis states that during periods of strong downwelling in the GoA, the influence of the Alaska Coastal Current, which flows westerly along the GoA continental margin (Weingartner et al., 2005), on PWS is stronger and more "river-like" with enhanced flushing, conversely during periods of weak downwelling, the ACC's influence on PWS is weaker and more "lake-like" with greater retention of water (Cooney et al., 2001a; Kline, 1999b).

To date, the herring population of PWS remains an injured resource from the *Exxon Valdez* oil spill, as the population biomass has remained at or below ~20,000 mt since 1998 and continues below this level that would allow a commercial catch (Muradian et al., 2017). Survival of juvenile (age-0) herring through their first winter is considered a potential factor limiting strong recruitment to the spawning population, and has therefore been the focus of past and ongoing research. Herring build energy reserves through the fall to fuel their metabolism during winter's low food abundance (Norcross et al., 2001), making environmental drivers of fall energy levels of particular interest. Here, we examine spatial and temporal variability in early and late winter measures of energy density among juvenile herring collected since 2007 as part of the PWS Herring Survey (pilot work 2007–2008, 2009–2011) and the PWS Herring Research and Monitoring Program (2012–2016) supported by long-term funding through the *Exxon Valdez* Oil Spill Trustee Council.

Following the SEA program's "river-lake" hypothesis, we tested the idea that oceanographic exchange between the northern GoA and PWS control juvenile herring nutritional processes and therefore the quality of these young forage fish. Similar to previous studies, our work relies on stable isotope gradients previously established between the GoA and PWS (e.g., Kline, 1999a, 1999b; Kline, 2009). Our work takes a relatively simple multi-model approach to understanding spatial and temporal variability in early (November) and late (March) winter measures of energy density by considering factors such as distinct hydrological regions of PWS related to circulation (space), year (time), either $\delta^{13}C$ or $\delta^{15}N$ signatures of fish tissues (trophic linkages) to assess either carbon source or relative trophic position, as well as interactions among these variables. We evaluate the same candidate models for both early and late winter measures of energy density to reveal seasonal differences in important explanatory variables.

2. Materials and methods

2.1. Study area

Prince William Sound, Alaska is a hydrographically complex, fjord-estuary located at the northern extent of the GoA (Fig. 1) that ranges in depth to nearly 800 m in the northwestern passage (Fig. 1; Halverson et al., 2013b; Niebauer et al., 1994). The Chugach National Forest, a mountainous temperate rainforest including numerous ice fields and tidewater glaciers, surrounds the region. Given the coastal rainforest climate, freshwater input from precipitation and glacial runoff is significant and varies seasonally with major contributions occurring in late summer and early fall (Beamer et al., 2016; Royer, 1979). To the south,

several large islands define the primary oceanographic conduits through which local PWS waters interact with the GoA, namely Hinchbrook Entrance (HE) and Montague Straight (MS; Fig. 1). The Alaska Coastal Current (ACC), which flows westerly along the GoA continental margin, and the Alaskan Stream (AS), which extends from the northern Gulf of Alaska to the western Aleutians just beyond the shelf break (Johnson et al., 1988; Royer, 1979; Stabeno and Reed, 1991; Weingartner et al., 2005) are the primary external oceanographic forces that influence PWS circulation and regional marine ecology (Cooney et al., 2001a; Eslinger et al., 2001; Kline, 1999b; Niebauer et al., 1994). General circulation of PWS, which flows cyclonically east to west, is highly seasonally influenced by interactions between the ACC and AS, freshwater input, and wind intensity. For example, during winter, strong easterly winds associated with the Aleutian low drive coastal downwelling over the continental shelf resulting in greater forcing of surface waters into PWS through HE that circulate cyclonically east to west and exit through MS (Cooney et al., 2001a; Halverson et al., 2013a; Niebauer et al., 1994). Conversely, during summer, the high pressure in the North Pacific causes a relaxation or even reversal of the downwelling allowing subsurface dense water to rise and transit into PWS through the bottom layer (Cooney et al., 2001a; Halverson et al., 2013a; Niebauer et al., 1994). Summertime surface flow in PWS becomes complex due to the addition of freshwater, which can result in eddies and current reversals (Vaughan et al., 2001; Wang et al., 2001).

2.2. Field sampling

Juvenile herring (age-0) were collected from a total of 19 nursery bays in PWS during research cruises in November, and by contracted commercial herring fisherman in March, of each year between 2007 and 2016 using cast and gill nets, or trawl gear. In November, fish were caught at night with field operations generally occurring around the new moon. Samples were collected using a midwater trawl where groups of fish were targeted during acoustic surveys of each bay. At times, deck lights were used to attract herring that were collected by cast and gill net along-side the research vessel as these gear types do not sample effectively at depth. Cast and gill net samples were taken to primarily compare with trawl caught samples. Although the use of deck lights might have imposed a bias by attracting more poor condition fish eager to feed, the spread of juvenile herring energy values collected by cast and gill nets spanned that of fish collected by trawl. Thus, capture methods are not expected to impose any bias on the energetic quality of the fish sampled during this study. In March, fish were caught using fisherman gill nets only. Nursery bays sampled during the SEA program were again sampled (i.e. Simpson, Eaglek, Whale and Zaikof Bays), in addition to many others including Cordova Harbor, Windy Bay, Double Bay, Port Gravina, Port Fidalgo, Valdez Arm, Jackson Hole (Glacier Island), Unakwik, West Twin Bay (Perry Island), Northwest Bay (Knight Island), Main Bay, Paddy Bay, Lower Herring Bay, Port Chalmers, and Port Etches (Fig. 1). Not all bays were sampled each year. Upon capture, fish were frozen in groups of 25–50 per sampling location and saved for laboratory processing at Prince William Sound Science Center in Cordova, Alaska.

2.3. Stable isotope and bomb calorimetry methods

In the laboratory, frozen juvenile herring were thawed and wet mass (mg) obtained using an analytical balance (Mettler). Length of each fish was measured to the nearest mm. Otoliths were excised and saved for other analyses. Fish were oven-dried (60 °C) and the final whole body dry mass recorded. Dried herring were ground to a fine powder using a ball mill (Retsch). Approximately 0.1–0.2 mg from each powdered herring was loaded into a tin capsule. Loaded capsules were sent to the University of Alaska Fairbanks Stable Isotope Facility where carbon (C) and nitrogen (N) mass spectrometric analyses were performed. Resultant data for juvenile herring included %C, %N, $^{13}C/^{12}C$, and $^{15}N/^{14}N$ with the heavy to light isotope ratios reported using delta notation, $\delta^{13}C$ and $\delta^{15}N$, respectively, calculated using the following equation: $\delta^{13}C$ or $\delta^{15}N = ([R_{sample}/R_{standard}]-1) \times 1000$, where R_{sample} is the ratio of the heavy to light isotope for either $^{13}C/^{12}C$ or $^{15}N/^{14}N$, and $R_{standard}$ is the heavy to light isotope ratios for international standards – Vienna PeeDee Belemnite for carbon and atmospheric N2 (Air) for nitrogen. Percent C and N data were used to ascertain C/N atom ratios. The ratios of dry to wet mass and C to N atoms were used to determine whole body energy density (WBED) based on relationships derived from (Paul et al., 2001) and refined by (Kline, 2013) using the following equation: WBED (kJ/g wet mass) = $-2.90242 + 32.585 \times$ (dry/wet mass ratio) + $0.103514 \times$ C/N atom ratio (see also Kline and Campbell, 2010). Raw $\delta^{13}C$ data were mathematically corrected for lipid content using the method of McConnaughey and McRoy (1979); see also Kline and Campbell (2010). Lipid-corrected values of $\delta^{13}C$ are hereafter reported as $\delta^{13}C'$.

A semi-micro calorimeter (Parr Instruments, model 6725) was used to perform bomb calorimetry (Parr Instrument Company, 2009) on a subset (~10%) of dried herring samples analyzed for $\delta^{13}C$ and $\delta^{15}N$ stable isotopes to ground-truth energy density estimates from dry/wet and C/N ratios. Although it was expected that estimates of WBED derived from dry/wet and C/N ratios would tightly correlate with energy density estimates derived from bomb calorimetry (e.g., Kline and Campbell, 2010), we explored these relationships for both November and March.

2.4. Statistical analyses

All analyses were restricted to juvenile herring up to 115 mm in fork length that were collected over nine years in November (2007–2015, $n = 2514$) and March (2008–2016, $n = 1889$). Nursery bay collection areas were grouped into four hydrological regions (central, north, west, and east regions, Fig. 1) following descriptions by Musgrave et al. (2013). However, the analyses presented here considered north and west regions separately, and did not include a Gulf of Alaska region, unlike Musgrave et al. (2013). All statistical analyses were performed in the R language environment version 3.4.1 (2017).

Least-squares linear models (lm function in R, hereafter linear models) were used to account for variation in WBED derived from stable isotope data for both November ($n = 258$) and March ($n = 253$). Two candidate models were considered for both November and March including an equal-means (null) model and a model with WBED derived from bomb calorimetry.

Two separate analyses were conducted to understand spatial and temporal variation in November WBED of age-0 herring in PWS (see Appendix A for a complete description of all explanatory variables and candidate models considered in analyses). First, linear mixed-effects models, employed using the lme function within the nlme package in R (Pinheiro et al., 2017, hereafter mixed models), were used to examine continuous variation in WBED derived from stable isotope data in relation to four parameters treated as fixed main effects including (1) fork length as a measure of body size (continuous variable); (2) $\delta^{13}C'$ stable isotope signature of age-0 herring (continuous variable) to assess carbon source; (3) nursery bay hydrological region in PWS (categorical variable – central, north, west, and east); and (4) year (categorical variable). Second, mixed models were again used to examine variation in November WBED in relation to three of these same parameters, fork length, nursery bay hydrological region, and year, but also $\delta^{15}N$ stable isotope signatures of age-0 herring as a continuous variable to assess trophic foraging. An *a priori* set of 10 candidate models were considered for each November analysis, including either $\delta^{13}C'$ or $\delta^{15}N$ stable isotope signatures, which consisted of a null model; models for isotope, region, or year predictor variables as fixed main effects including a term for fork length to control for body size in each model (three models); a more complex multiple predictor model including fixed main effect terms for fork length, isotope, and region (one model). All models

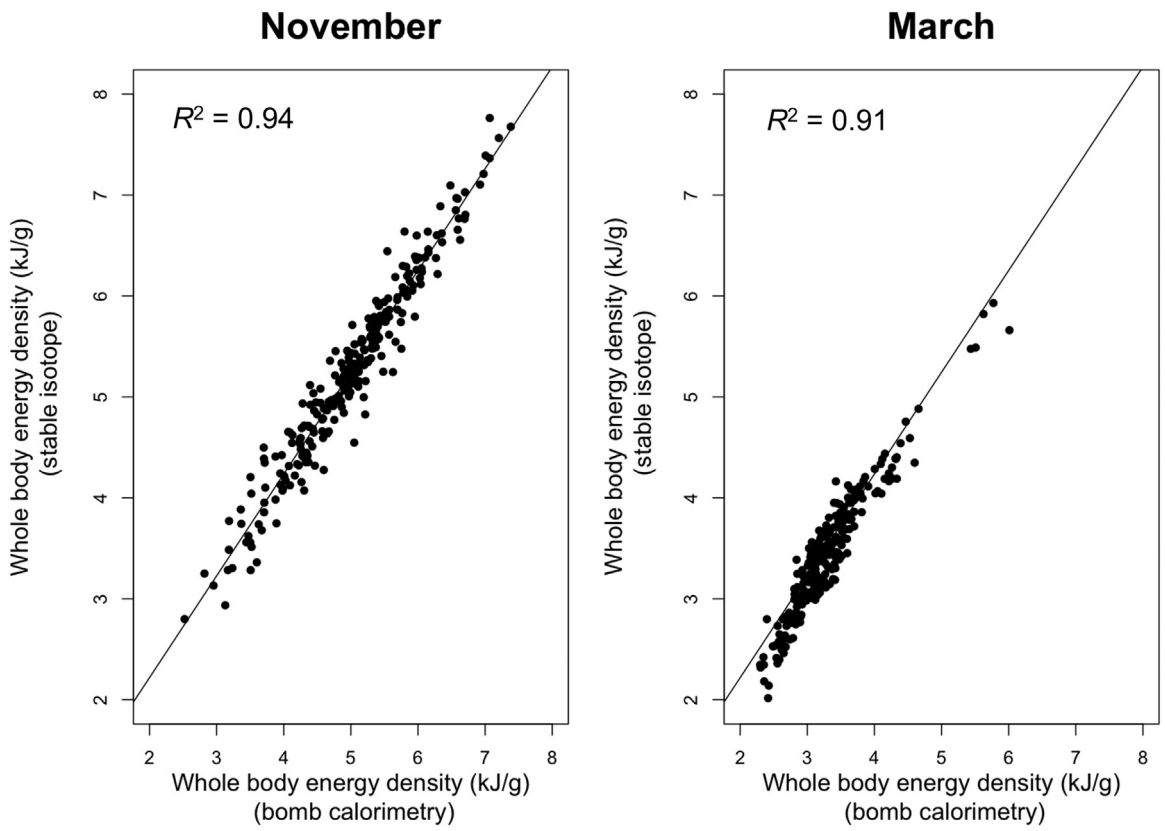

Fig. 2. Variation in November and March whole body energy density of juvenile Pacific herring derived from stable isotope data in relation to whole body energy density derived from bomb calorimetry.

without a year term were further evaluated including a year term (three models). Additional interaction models were included: a global model with all four fixed main effects and an interaction between isotope signature and region, and a second global model with all four fixed main effects and an interaction between isotope signature and year (two models). A random effect on intercept and slope (random = ~1 + Fork Length|Collection Bay) was included in each model to control for non-independence of data given that some fish were collected from the same nursery bay, and therefore, experienced more similar local environmental conditions that might have influenced individual size and energetic status.

Similarly, two separate analyses were conducted to understand spatial and temporal variation in March WBED derived from stable isotope data of age-0 herring in PWS. Again, mixed models included the same explanatory variables and candidate model sets describe for November analyses (Appendix A).

For November and March WBED analyses, the importance of including a random effect on intercept and slope was tested in preliminary analyses by comparing the fit of four models, based on Akaike's Information Criterion corrected for small sample size (AICc), for each analysis - the most parameterized fixed effect model without a random effect (using the gls function in R), with a random effect on intercept only (mixed model), with a random effect on slope only (mixed model), and with a random effect on both intercept and slope (mixed model). All four models maximized the restricted log-likelihood (method = "REML") and all models included the same fixed main effect parameters and their interaction. The most parameterized fixed effect model with a random effect on both intercept and slope received the lowest AICc value for each analysis. Therefore, a random effect on both intercept and slope was included in all candidate models for November and March analyses.

Information-theoretic methods were used to direct model selection and parameter estimation (Burnham and Anderson, 2002). For each candidate model, AICc, ΔAICc and Akaike weight (w) values were calculated using the AICcmodavg package in R (Mazerolle, 2017) and used to compare models (Burnham and Anderson, 2002). Values for ΔAICc are scaled differences relative to the smallest AICc value in the candidate model set such that the model with the minimum AICc value has $\Delta_i = 0$ (Burnham and Anderson, 2002). Values for Akaike weights are the relative likelihood of the model, given the data, normalized to sum to 1 and interpreted as probabilities (Burnham and Anderson, 2002). Inference was based on the relative support for parameters across all models and weighted parameter estimates. Parameter estimation included calculation of model-averaged parameter estimates based on w values for all candidate models within a candidate model set. Standard errors (SE) and 95% confidence intervals (CI: SE*1.96) for parameter estimates were based on unconditional variances calculated across the same models. Parameter likelihood values were evaluated by summing w values across all models that included each parameter under consideration (Burnham and Anderson, 2002). Ultimately, only two models were considered in comparing stable isotope and bomb calorimetry estimates of WBED, including the null model, therefore no model averaging calculations were conducted for this analysis.

Linear models were used to compare stable isotope and bomb calorimetry estimates of WBED, thus an R^2 value defined as the fraction of the total variance explained by the model, was calculated as a general measure of fit (see Crawley, 2007, p. 399). For mixed models, a pseudo R^2 value was calculated following Xu (2003), which is defined as 1 - the residual variance of the full model / the residual variance of a null model. Best supported models for November and March WBED analyses were examined based on standardized residual versus fitted value plots and normal probability plots of residuals to further assess model fit.

3. Results

Models including WBED derived from bomb calorimetry were best

Table 1
Candidate models describing variation in whole body energy density of juvenile Pacific herring in Prince William Sound, Alaska. Models presented are those determined to be most parsimonious, as well all models receiving ΔAICc values ≤ 2.

Month and isotope	Response variable	Model number	Explanatory variables	Number of parameters	ΔAICc	*w*	*Pseudo* R^2
November, $\delta^{13}C'$	WBED (kJ/g)	9	FL + $\delta^{13}C'$ + Region + Year + $\delta^{13}C'$*Region, random = ~1 + FL|Collection Bay	21	0.00	0.99	0.26
November, $\delta^{15}N$	WBED (kJ/g)	9	FL + $\delta^{15}N$ + Region + Year + $\delta^{15}N$*Region, random = ~1 + FL|Collection Bay	21	0.00	1.00	0.23
March, $\delta^{13}C'$	WBED (kJ/g)	10	FL + $\delta^{13}C'$ + Region + Year + $\delta^{13}C'$*Year, random = ~1 + FL|Collection Bay	26	0.00	1.00	0.22
March, $\delta^{15}N$	WBED (kJ/g)	10	FL + $\delta^{15}N$ + Region + Year + $\delta^{15}N$*Year, random = ~1 + FL|Collection Bay	26	0.00	1.00	0.20

Abbreviations: ΔAICc = Akaike's Information Criterion corrected for small sample size, *w* = Akaike weight, WBED = whole body energy density, FL = fork length, $\delta^{13}C'$ = lipid corrected carbon stable isotope signature, $\delta^{15}N$ = nitrogen stable isotope signature.

supported (November: ΔAICc value = 0.00, March: ΔAICc value = 0.00) over null models for describing variation in both November and March WBED where values were derived from dry/wet mass and C/N atom ratios of juvenile herring. Each model received very high weight and goodness of fit values (November: $w = 1.00$, $R^2 = 0.94$; March: $w = 1.00$, $R^2 = 0.91$; Fig. 2). Estimates of WBED based on stable isotope data were considered reliable because of these strong relationships and consequently used in the analyses reported below.

3.1. November

Only one model including $\delta^{13}C'$ stable isotope signatures received a ΔAICc value ≤ 2.00 for describing variation in November WBED, which included all terms as fixed main effects (fork length, $\delta^{13}C'$ isotope signature, hydrological region, and year), as well as an interaction between $\delta^{13}C'$ isotope signature and region (Appendix A: carbon stable isotope analysis for November, model 9). Plots of standardized residual versus fitted values and normal probability plots of residuals indicated model 9 was fitted adequately. This best-supported model received a high *w* value (0.99), but only explained 26% of the variation in the data (Table 1). Parameter likelihoods indicated strong support for all fixed main effect parameters and the interaction between $\delta^{13}C'$ isotope signature and region (1.00, Table 2). The interaction between $\delta^{13}C'$ isotope signature and year was not supported (3.98 E-15, Table 2). Fish with larger body sizes were more energy dense (0.02 ± 0.01 CI, Table 2). Fish with more depleted $\delta^{13}C'$ isotope signatures were more energy dense (−0.16 ± 0.09 CI, Table 2). The interaction between $\delta^{13}C'$ isotope signature and region was strongest in the west (−0.38 ± 0.10 CI) and north (−0.14 ± 0.12 CI) where fish with a more depleted $\delta^{13}C'$ stable isotope signature were more energy dense (Table 2, Fig. 3). Juvenile herring caught in the fall of 2013 (0.30 ± 0.16 CI) were the most energy dense, while fish caught in the fall of 2015 were the least energy dense (−1.07 ± 0.19 CI, Table 2, Fig. 3). See Supplemental material Fig. 1 for plots of WBED versus $\delta^{13}C'$ stable isotope signatures for November.

Only one model including $\delta^{15}N$ stable isotope signatures received a ΔAICc value ≤ 2.00 for describing variation in November WBED, which included all terms as fixed main effects (fork length, $\delta^{15}N$ isotope signature, hydrological region, and year), as well as an interaction between $\delta^{15}N$ isotope signature and region (Appendix A: nitrogen stable isotope analysis for November, model 9). Plots of standardized residual versus fitted values and normal probability plots of residuals indicated model 9 was fitted adequately. This best-supported model received a high *w* value (1.00), but again only explained 23% of the variation in the data (Table 1). Parameter likelihoods indicated strong support for all fixed main effect parameters and the interaction between $\delta^{15}N$ isotope signature and region (0.99–1.00, Table 2). Again, the interaction between $\delta^{15}N$ isotope signature and year was not supported (4.53 E-07, Table 2). Fish with larger body sizes were more energy dense (0.02 ± 0.01 CI, Table 2). Fish from northern nursery bays were more energy dense (2.88 ± 2.31 CI, Table 2). The interaction between $\delta^{15}N$ isotope signature and region was strongest in the north (−0.26 ± 0.19 CI) where fish with a more depleted $\delta^{15}N$ isotope signature were more energy dense (Fig. 4). Juvenile herring caught in the fall of 2012 were the most energy dense (0.86 ± 0.15 CI), while fish caught in the fall of 2015 were the least energy dense (−0.41 ± 0.16 CI, Table 2, Fig. 4). See Supplemental material Fig. 2 for plots of WBED versus $\delta^{15}N$ stable isotope signatures for November.

3.2. March

Only one model including $\delta^{13}C'$ stable isotope signatures received a ΔAICc value ≤ 2.00 for describing variation in March WBED, which included all terms as fixed main effects (fork length, $\delta^{13}C'$ isotope signature, hydrological region, and year), as well as an interaction between $\delta^{13}C'$ isotope signature and year (Appendix A: carbon stable isotope analysis for March, model 10). Plots of standardized residual versus fitted values and normal probability plots of residuals indicated model 10 was fitted adequately. This best-supported model received a high *w* value (1.00), but only explained 22% of the variation in the data (Table 1). Parameter likelihoods indicated strong support for all fixed main effect parameters and the interaction between $\delta^{13}C'$ isotope signature and year (1.00, Table 2). The interaction between $\delta^{13}C'$ isotope signature and region was not supported (8.07 E-20, Table 2). Again, fish with larger body sizes were more energy dense (0.02 ± 0.01 CI, Table 2). The interaction between $\delta^{13}C'$ isotope signature and year was strongest for fish caught in 2016 (−1.42 ± 0.38 CI, Fig. 5) where individuals with a more depleted $\delta^{13}C'$ isotope signature were more energy dense (Fig. 5). See Supplemental material Fig. 3 for plots of WBED versus $\delta^{13}C'$ stable isotope signatures for March.

Similar to other analyses, only one model including $\delta^{15}N$ stable isotope signatures received a ΔAICc value ≤ 2.00 for describing variation in March WBED, which included all terms as fixed main effects (fork length, $\delta^{15}N$ isotope signature, hydrological region, and year), as well as an interaction between $\delta^{15}N$ isotope signature and year (Appendix A: nitrogen stable isotope analysis for March, model 10). Plots of standardized residual versus fitted values and normal probability plots of residuals indicated model 10 was fitted adequately. This best-supported model received a high *w* value (1.00), but only explained 20% of the variation in the data (Table 1). Parameter likelihoods indicated strong support for all main effect parameters and the interaction between $\delta^{15}N$ isotope signature and year (1.00, Table 2). The interaction between $\delta^{15}N$ isotope signature and region was not supported (1.83 E-09, Table 2). Fish with larger body sizes were more energy dense (0.02 ± 0.01 CI, Table 2). The interaction between $\delta^{15}N$ isotope signature and year was strongest for fish caught in 2016 (−0.57 ± 0.44, Table 2) where juvenile herring with more depleted $\delta^{15}N$ isotope signatures were more energy dense (Fig. 5). See Supplemental material Fig. 4 for plots of WBED versus $\delta^{15}N$ stable isotope signatures for March.

Table 2
Parameter estimates and likelihoods from candidate models for describing variation in November and March whole body energy density of juvenile Pacific herring in Prince William Sound, Alaska. Parameter estimates (± 95% confidence intervals) are weighted averages. Parameter likelihoods are Akaike weight (*w*) values summed across all models that include the variable. Results are presented for A) candidate models including $\delta^{13}C'$ and B) candidate models including $\delta^{15}N$.

A) Parameters from candidate models including $\delta^{13}C'$

Response variable	Explanatory variables	Parameter likelihoods		Parameter estimates ± CI	
		November	March	November	March
WBED (kJ/g)	Intercept	1.00	1.00	0.38 ± 2.14	5.73 ± 5.49
	FL	1.00	1.00	0.02 ± 0.01	0.02 ± 0.01
	$\delta^{13}C'$	1.00	1.00	−0.16 ± 0.09	0.22 ± 0.29
	Location-East	1.00	1.00	1.13 ± 2.00	−0.02 ± 0.14
	Location-North	1.00	1.00	−3.07 ± 2.44	−0.11 ± 0.15
	Location-West	1.00	1.00	−7.75 ± 2.17	−0.02 ± 0.15
	Year2008/09[a]	1.00	1.00	−0.38 ± 0.23	−1.50 ± 6.80
	Year2009/10[a]	1.00	1.00	−0.26 ± 0.20	−4.43 ± 5.86
	Year2010/11[a]	1.00	1.00	−0.51 ± 0.17	−2.54 ± 5.79
	Year2011/12[a]	1.00	1.00	0.02 ± 0.16	−3.87 ± 5.67
	Year2012/13[a]	1.00	1.00	0.19 ± 0.20	0.02 ± 6.48
	Year2013/14[a]	1.00	1.00	0.30 ± 0.16	−5.80 ± 5.81
	Year2014/15[a]	1.00	1.00	−0.22 ± 0.17	−5.83 ± 6.16
	Year2015/16[a]	1.00	1.00	−1.07 ± 0.19	−28.01 ± 7.29
	$\delta^{13}C'$*LocationEast	1.00	8.07 E−20	0.08 ± 0.10	−5.71 E−21 ± 2.49 E−20
	$\delta^{13}C'$*LocationNorth	1.00	8.07 E−20	−0.14 ± 0.12	−6.98 E−21 ± 3.02 E−20
	$\delta^{13}C'$*LocationWest	1.00	8.07 E−20	−0.38 ± 0.10	−1.04 E−20 ± 4.25 E−20
	$\delta^{13}C'$*Year2008/09[a]	3.89 E−15	1.00	−1.16 E−15 ± 5.06 E−15	−0.07 ± 0.36
	$\delta^{13}C'$*Year2009/10[a]	3.89 E−15	1.00	−1.50 E−15 ± 6.17 E−15	−0.22 ± 0.31
	$\delta^{13}C'$*Year2010/11[a]	3.89 E−15	1.00	5.95 E−18 ± 1.10 E−15	−0.13 ± 0.31
	$\delta^{13}C'$*Year2011/12[a]	3.89 E−15	1.00	6.15 E−17 ± 1.08 E−15	−0.20 ± 0.30
	$\delta^{13}C'$*Year2012/13[a]	3.89 E−15	1.00	−3.83 E−16 ± 2.04 E−15	−0.05 ± 0.34
	$\delta^{13}C'$*Year2013/14[a]	3.89 E−15	1.00	−3.16 E−16 ± 1.85 E−15	−0.29 ± 0.31
	$\delta^{13}C'$*Year2014/15[a]	3.89 E−15	1.00	−2.43 E−16 ± 1.58 E−15	−0.31 ± 0.33
	$\delta^{13}C'$*Year2015/16[a]	3.89 E−15	1.000	−1.78 E−15 ± 7.15 E−15	−1.42 ± 0.38

B) Parameters from candidate models including $\delta^{15}N$

Response variable	Explanatory variables	Parameter likelihoods		Parameter estimates ± CI	
		November	March	November	March
WBED (kJ/g)	Intercept	1.00	1.00	5.09 ± 2.18	0.40 ± 4.40
	FL	1.00	1.00	0.02 ± 0.01	0.02 ± 0.01
	$\delta^{15}N$	1.00	1.00	−0.14 ± 0.16	0.11 ± 0.36
	Location-East	0.99	1.00	0.59 ± 2.28	−0.07 ± 0.10
	Location-North	0.99	1.00	2.88 ± 2.31	−0.17 ± 0.11
	Location-West	0.99	1.00	−1.99 ± 2.58	−0.08 ± 0.11
	Year2008/09[a]	1.00	1.00	0.14 ± 0.22	−1.33 ± 6.79
	Year2009/10[a]	1.00	1.00	−0.02 ± 0.19	2.96 ± 4.57
	Year2010/11[a]	1.00	1.00	−0.23 ± 0.16	−1.68 ± 4.52
	Year2011/12[a]	1.00	1.00	0.42 ± 0.15	−1.67 ± 4.64
	Year2012/13[a]	1.00	1.00	0.86 ± 0.15	2.54 ± 4.82
	Year2013/14[a]	1.00	1.00	0.32 ± 0.17	2.32 ± 4.42
	Year2014/15[a]	1.00	1.00	0.14 ± 0.15	2.19 ± 4.58
	Year2015/16[a]	1.00	1.00	−0.41 ± 0.16	6.93 ± 5.32
	$\delta^{15}N$*LocationEast	0.99	1.83 E−09	−0.07 ± 0.18	3.64 E−10 ± 1.46 E−09
	$\delta^{15}N$*LocationNorth	0.99	1.83 E−09	−0.26 ± 0.19	5.20 E−11 ± 3.45 E−10
	$\delta^{15}N$*LocationWest	0.99	1.83 E−09	0.17 ± 0.21	1.45 E−11 ± 2.72 E−10
	$\delta^{15}N$*Year2008/09[a]	4.53 E−07	1.00	1.71 E−08 ± 1.99 E−07	0.07 ± 0.54
	$\delta^{15}N$*Year2009/10[a]	4.53 E−07	1.00	1.06 E−07 ± 4.92 E−07	−0.27 ± 0.37
	$\delta^{15}N$*Year2010/11[a]	4.53 E−07	1.00	−1.42 E−08 ± 1.86 E−07	0.12 ± 0.37
	$\delta^{15}N$*Year2011/12[a]	4.53 E−07	1.00	1.71 E−09 ± 1.55 E−07	0.13 ± 0.38
	$\delta^{15}N$*Year2012/13[a]	4.53 E−07	1.00	1.16 E−07 ± 4.98 E−07	−0.16 ± 0.40
	$\delta^{15}N$*Year2013/14[a]	4.53 E−07	1.00	2.50 E−08 ± 1.87 E−07	−0.22 ± 0.36
	$\delta^{15}N$*Year2014/15[a]	4.53 E−07	1.00	3.12 E−08 ± 2.25 E−07	−0.18 ± 0.38
	$\delta^{15}N$*Year2015/16[a]	4.53 E−07	1.00	−1.77 E−08 ± 1.95 E−07	−0.57 ± 0.44

Abbreviations: ± CI = plus or minus 95% confidence interval, WBED = whole body energy density, FL = fork length, $\delta^{13}C'$ = lipid corrected carbon stable isotope signature, $\delta^{15}N$ = nitrogen stable isotope signature.

[a] Signifies a parameter including Year, or an interaction with Year, where the first year noted is for November and the second year for March, i.e., parameters estimates for Year 2008/09 would be for November 2008 and March 2009, respectively.

4. Discussion

Our study identified important factors influencing the WBED of juvenile Pacific herring in PWS, Alaska for fish sampled in early and late winter. For November analyses, a strong negative relationship between WBED and the $\delta^{13}C'$ isotope signature of fish, particularly those collected from the northern and western regions of PWS, indicated that fish with a more depleted $\delta^{13}C'$ isotope signature were more energy dense (Fig. 3, Supplemental material Fig. 1). This is an interesting result given previous work on isotopic gradients between the GoA and PWS, which indicated that while there is some overlap, $\delta^{13}C'$ values of *N. cristatus* collected from the GoA ranged from −27‰ to −17‰, while $\delta^{13}C'$ values for *N. cristatus* collected from PWS ranged from −23‰ to −17‰ with $\delta^{13}C'$ values of −21‰ to 20‰ representing an approximate demarcation between carbon derived from the GoA and PWS, respectively (see Kline, 2009 Figure 7). Our $\delta^{13}C'$ isotope data for November ranged approximately from −24‰ to −17‰ across all regions of PWS (Supplemental material Fig. 1). However, in both the northern

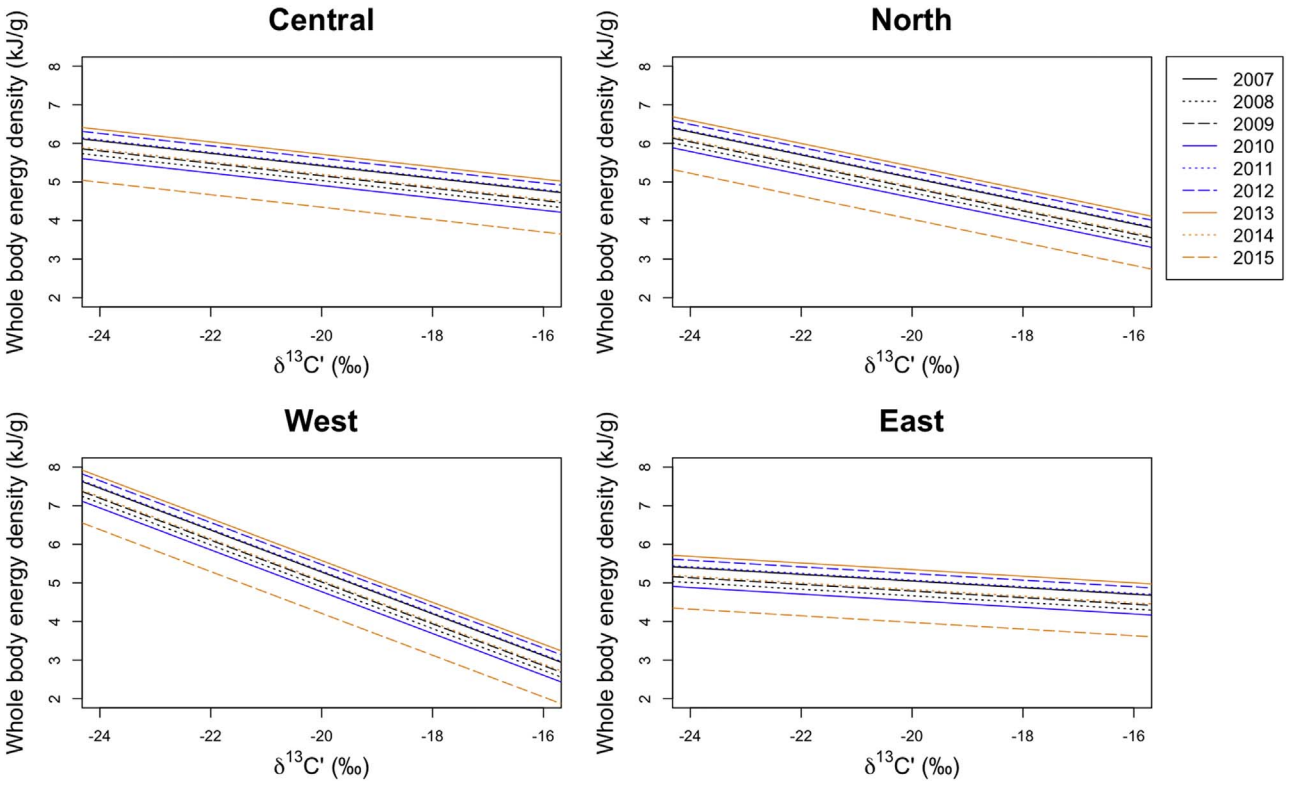

Fig. 3. Modeled variation in November whole body energy density of juvenile Pacific herring of Prince William Sound, Alaska in relation to $\delta^{13}C'$, hydrological region, and year. Regressions are based on weighted parameter estimates across all models for the average size herring and range of $\delta^{13}C'$ values (−23.46 to −16.82) for samples collected in November.

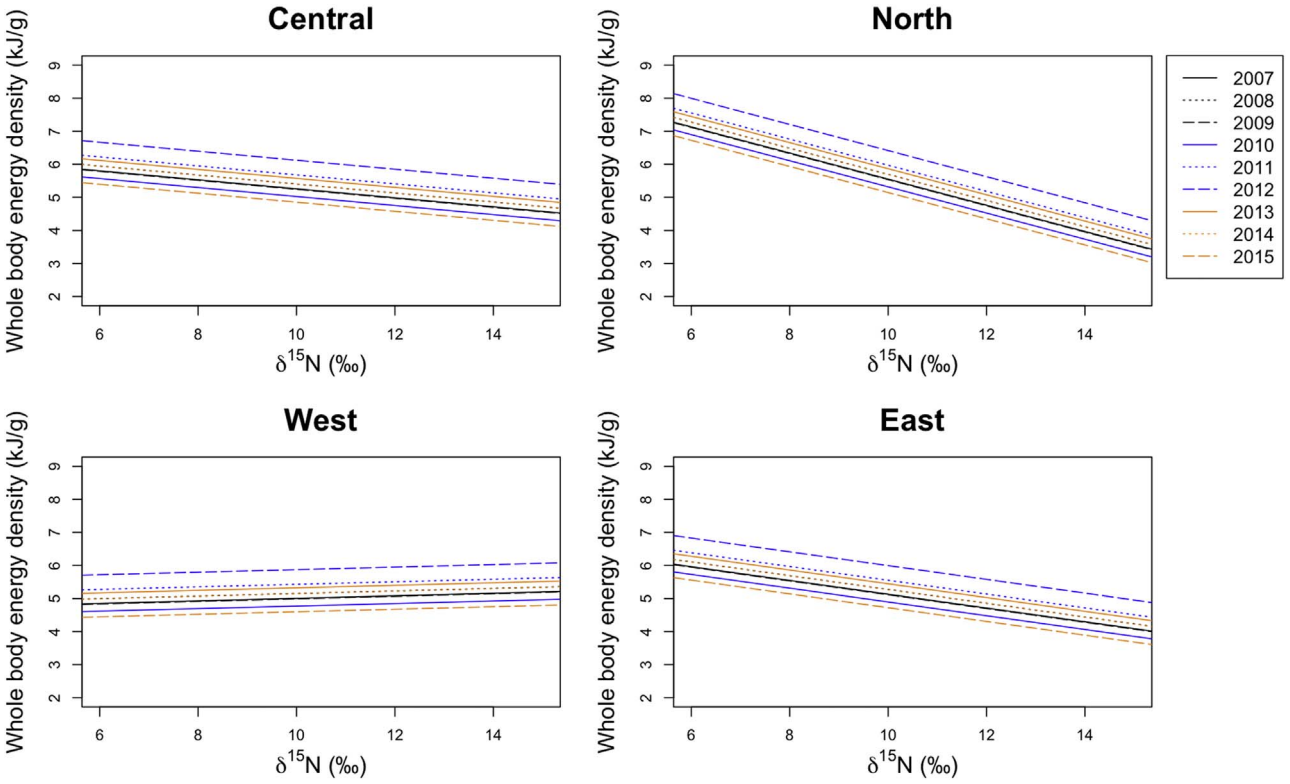

Fig. 4. Modeled variation in November whole body energy density of juvenile Pacific herring of Prince William Sound, Alaska in relation to $\delta^{15}N$, hydrological region, and year. Regressions are based on weighted parameter estimates across all models for the average size herring and range of $\delta^{15}N$ values (6.79–14.55) for samples collected in November.

and western regions of PWS, $\delta^{13}C'$ data appear to be marginally skewed towards more depleted $\delta^{13}C'$ values, particularly in comparison with data from the eastern region (Supplemental material Fig. 1). We interpret these findings as evidence that carbon derived from the GoA ($\delta^{13}C' < -20.5$‰) enhances the early winter quality of juvenile herring in PWS, particularly in the northern and western regions of PWS.

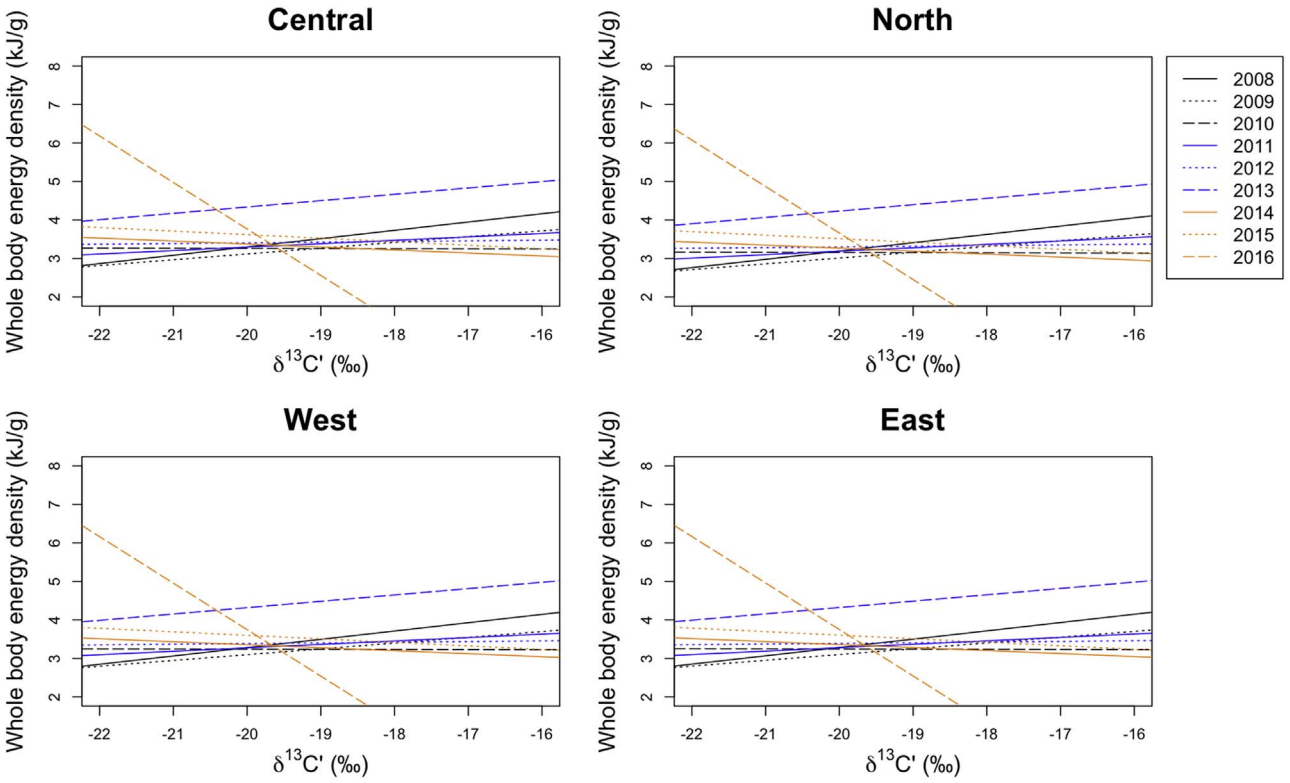

Fig. 5. Modeled variation in March whole body energy density of juvenile Pacific herring of Prince William Sound, Alaska in relation to $\delta^{13}C'$, hydrological region, and year. Regressions are based on weighted parameter estimates across all models for the average size herring and range of $\delta^{13}C'$ values (−22.06 to −16.78) for samples collected in March.

Earlier studies did not consider carbon source as a potential correlate of juvenile herring quality (Kline, 1997, 1999a, 1999b, 2000, 2001; Paul and Paul, 1999). Our demonstration of the interaction between $\delta^{13}C'$ value and hydrological region of PWS indicates a role for oceanographic exchange with the GoA operating on the quality of juvenile herring. In November, fish collected from the eastern region were less energy dense than fish collected from other regions (central, northern and western, Table 2). The central, northern and western regions of PWS are all areas characterized by deep bathymetry associated with a marine canyon that extends from the continental shelf into PWS that follows a cyclonic east to west trajectory (Fig. 1). Water from the GoA flows into PWS through this marine canyon and its distribution in the region is determined by bathymetry, particularly in the summer and early fall when downwelling is relaxed and deep water more easily transits into PWS through the bottom layer (Cooney et al., 2001b; Halverson et al., 2013a). Thus, it is not surprising that the regions in PWS associated with deep bathymetry and an expected influx of water from the GoA also produce juvenile herring that hold a GoA carbon signature that are more energy dense, particularly in early winter (Figs. 1 and 3). Interestingly, earlier studies by Paul and Paul (1999) demonstrated that WBED of juvenile herring collected from areas such as Eaglek, Whale and Zaikof Bays in the northern, western and central regions of PWS, respectively, were not different from each other, however, juvenile herring collected from Simpson Bay in the eastern region had lower WBED values than fish from these other areas. Their study was conducted across only three years (1995–1997), however, coupled with our results it appears that these regional dynamics in herring WBED are mainly consistent.

We are intrigued by the finding that although $\delta^{13}C'$ data appear to be marginally skewed towards more depleted $\delta^{13}C'$ values in the northern and western regions of PWS, the range of $\delta^{13}C'$ values across all regions is not that dramatically different. However, there is clearly a stronger relationship between $\delta^{13}C'$ and WBED in the northern and western regions of PWS (Fig. 3; Supplemental material Fig. 1). This suggests to us that there may be different transport mechanisms driving relationships between $\delta^{13}C'$ and WBED of PWS juvenile herring possibly in the context of different zooplankton communities and abundance associated with different hydrological regions of PWS. Early studies identified *Neocalanus, Calanus, and Pseudocalanus* copepods overwintering (October and November) in areas deeper than ~400 m in PWS in preparation for reproduction in January and February (Damkaer, 1977; Eslinger et al., 2001). These deep areas of PWS therefore provide excellent reproductive habitat for these species elevating their densities relative to other areas of the GoA shelf (Cooney, 1986). Research conducted during the years of the current study confirmed that in some years large calanoids can comprise up to 50% of the diet of juvenile herring in early winter (Gorman et al., 2017). Thus, we suggest the relationship between $\delta^{13}C'$ and WBED of PWS juvenile herring might be driven by differing zooplankton communities with variable energetic qualities and/or abundances dominating the various hydrological regions of PWS, providing a transport mechanism for GoA carbon to influence juvenile herring quality.

During the fall, a negative relationship between WBED and $\delta^{15}N$ isotope signature was observed in the northern region of PWS (Fig. 4) indicating that fish feeding on relatively lower trophic level prey were more energy dense. Isotopic studies of zooplankton in PWS have additionally indicated that prey such as copepods are depleted in $\delta^{15}N$ relative to other dominant prey such as amphipods and euphausiids (Kline, 1999b). The diets of juvenile herring in the northern region of PWS might have primarily consisted of copepods, which corroborates our thinking in terms of $\delta^{13}C'$ variability and would explain feeding at relatively lower trophic levels.

Results for $\delta^{13}C'$ stable isotopes indicate that carbon source is more strongly related to WBED in the fall than in the spring (Figs. 3 and 5), which likely reflects fish foraging more aggressively in the summer and fall to accumulate energy reserves for overwintering. Oceanographic exchange with GoA carbon suggests that ocean-climate conditions enhancing the intrusion of GoA water into PWS should have a positive

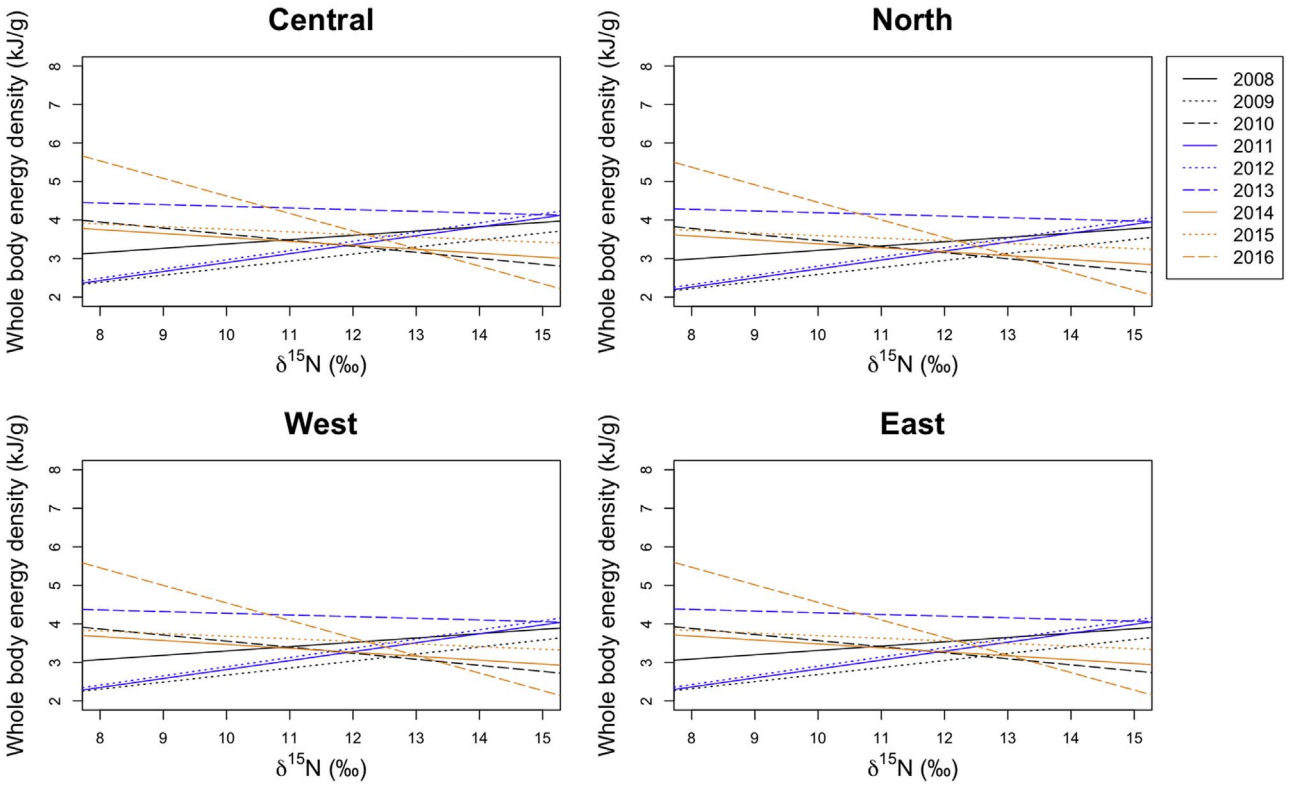

Fig. 6. Modeled variation in March whole body energy density of juvenile Pacific herring of Prince William Sound, Alaska in relation to $\delta^{15}N$, hydrological region, and year. Regressions are based on weighted parameter estimates across all models for the average size herring and range of $\delta^{15}N$ values (7.98–14.69) for samples collected in March.

effect on the quality of juvenile herring, particularly those intrusions that operate in the late summer and fall. The lack of a relationship in spring between WBED and the $\delta^{13}C'$ isotope signature of individual fish (Table 2, Fig. 5) suggests that some amount of local PWS feeding might be occurring during winter leading to isotope signatures of fish becoming slightly enriched. Winter-feeding by juvenile herring in Simpson Bay, PWS, has been suggested given observations of more enriched $\delta^{13}C'$ isotope signatures reflective of local PWS production (Gorman, Sewall and Heintz unpubl. data; see also Foy and Norcross, 1999; Kline and Campbell, 2010). Only in one year (2016) did the negative relationship between WBED and $\delta^{13}C'$ isotope signatures persist (Fig. 5). Environmental conditions were extremely warm in 2016 and it is possible that the spring bloom occurred earlier in 2016 providing fish with food resources typically found outside the late winter season.

Year was an important factor in both early and late winter analyses. In November, fish were most energy dense in 2012 and 2013, and least energy dense in 2015 (Figs. 3 and 4). In March, fish were the most energy dense in 2013 with all other years being rather similar in terms of energy density (Figs. 5 and 6). Interestingly, in early winter 2012 and 2015 fish were also the most depleted in $\delta^{13}C'$ of the nine-year time series (Supplemental material Fig. 1). Herring were also most depleted in March in 2013, but not in 2016 (Supplemental material Fig. 3). The opposing annual results between WBED and $\delta^{13}C'$ further suggests the possibility that yearly variation in WBED is ultimately driven by variation in zooplankton community structure and abundance influenced by GoA intrusion. One environmental factor that stands out between early and late winter 2012/13 and 2015/16 is temperature. The winter of 2012/13 was one of the coldest in the nine-year time series - November and December 2012 were the coldest November and December months since 2007, while January through March 2013 was relatively average for temperature (Cordova NOAA tide station data). Cold temperatures reduce the metabolism of fish, possibly making it easier to survive the winter. Accordingly, fish captured in the spring of 2013 were among the highest quality in the time series. The fall of 2015 occurred during a marked warming period in the GoA (Bond et al., 2015). Temperatures leading into the fall of 2015 were anomalously warm and associated with reduced quality of juvenile herring. Thus, even in the relatively short time series presented here, there appears to be links to water temperature regimes in PWS and the GoA, where cold environmental conditions enhance the energy density of fish, while warm environmental conditions reduce juvenile herring quality. We note, however, that temperature is one of many environmental factors that shape yearly conditions for juvenile herring. A recent study by Ward et al. (2017) noted freshwater discharge as an important factor influencing herring productivity in PWS before, during and after the *Exxon Valdez* oil spill. Further, the intensity of downwelling on the shelf is known to play a role in GoA intrusions into PWS with seasonal variability important to “river-lake” dynamics (Cooney et al., 2001a). However, we note that downwelling intensity has not consistently correlated with annual measures of spring zooplankton stocks (Eslinger et al., 2001).

It is interesting that the interaction between $\delta^{13}C'$ isotope signature and region was only supported for November analyses, while the interaction between $\delta^{13}C'$ isotope signature and year was supported for March analyses. This result leads us to highlight the important seasonal differences driving intrusion of water from the GoA into PWS that then shapes energy density of juvenile herring in the fall, and the likely scenario that winter-feeding by juvenile herring might enrich their tissues without considerable energy gain, thereby removing any relationship between WBED and $\delta^{13}C'$ isotope signature in the spring. Enhanced winter downwelling is predicted to make PWS more “river-like” flushing zooplankton out of the PWS system. Thus, it may not be surprising that juvenile herring foraging during winter may be relying more on local production than that from the GoA.

Lastly, larger fish were more energy dense during both early and late winter seasons. Our results generally follow those from early studies by Paul and Paul (1998) that showed larger fish, from older age

classes, are more energy dense. However, age-0 herring are thought to build nutrient reserves through their first fall that are used during overwinter while fasting when food availability is low (Blaxter and Holiday, 1963; Norcross et al., 2001; Paul et al., 1998). High temporal resolution studies have indicated that fish maximized their energy levels in November and energy is rapidly lost over the next one to two months, with energy maintained at minimum levels through March (Gorman, Sewall and Heintz, unpubl. data). Growth during winter appeared minimal, yet fish sampled in the spring were larger than those sampled in the fall (Gorman, Sewall and Heintz, unpubl. data), suggestive of size-dependent mortality (see also Foy and Norcross, 1999; Norcross et al., 2001; Paul et al., 1998). Our observation regarding the positive relationship between size and energy density of juvenile herring provides a plausible mechanism underlying overwinter size dependent mortality. Through experimental studies, Paul and Paul (1998) determined that captive juvenile herring that died from starvation had WBED values < 3.2 – 3.6 kJ/g wet weight. Our results show WBED of juvenile herring in March to range between 3 – 4 kJ/g wet mass (Figs. 5 and 6, Supplemental material Figs. 3 and 4), which is generally in the range detected by Paul and Paul (1998), and further supports the idea that juvenile herring in the spring appear to exist near the energetic limits that support life.

In summary, the quality of juvenile herring in PWS appears to be influenced by oceanographic exchange with the GoA that is facilitated by PWS bathymetry and circulation, in addition to local temperature regimes. Zooplankton community structure and abundance presumably act as important transport mechanisms for GoA carbon to PWS juvenile herring. The energetic condition of young herring is enhanced in the northern and western regions of PWS and during colder temperature regimes. Best-supported models for both November and March had relatively low pseudo R^2 values (0.20–0.26), highlighting that other factors must be important predictors of WBED for young herring. For this reason, it remains dubious whether oceanographic exchange with the GoA is driving energetic variability that influences juvenile herring production and recruitment to the spawning population. Links between GoA and PWS oceanographic exchange and juvenile herring recruitment would be better established by long-term coupled oceanographic (zooplankton community structure and abundance, as well as $\delta^{13}C$ and $\delta^{15}N$ stable isotopes) sampling in the GoA and PWS much like the work reported by Kline (2009), as well as modeling of these connections (Coyle et al., 2013). Other possible approaches include using isotope methods to compare the geochemical signature of otoliths between juvenile herring in the eastern and western/northern regions of PWS during their first summer growth phase and those of older, recruited herring (e.g., Walther et al., 2008). If a large proportion of the spawning population had otolith geochemical signatures from the first summer growth phase that are more similar to juveniles from a specific region of PWS, greater links between GoA/PWS oceanographic exchange and herring recruitment would be established.

Acknowledgements

We thank three anonymous reviewers, R. Hopcroft (guest editor), and K. Drinkwater (editor) for comments that greatly improved the manuscript. Captain D. Beam and crew of the F/V *Montague* assisted with fall collections of herring, while members of Cordova District Fishermen United assisted with spring collections. Several excellent field and lab technicians including K. Siwicke, J. Todd, K. Jurica, D. Roberts, J. McMahon, A. Potter, and V. Gonzalez assisted with field collections and sample processing for stable isotopes and bomb calorimetry. N. Haubenstock and T. Howe at the Alaska Stable Isotope Facility, University of Alaska Fairbanks, analyzed samples for carbon and nitrogen stable isotopes. We thank J. Maselko and T. Morgan for statistical advice, and A. Schaefer for assistance with mapping. Prince William Sound Science Center provided administrative and logistical support. We are especially grateful to the *Exxon Valdez* Oil Spill Trustee Council for long-term support of research on the energetics of juvenile herring in PWS. The findings and conclusions presented by the authors are their own and do not necessarily reflect the views or position of the Trustee Council.

Appendix A. Candidate model sets for describing variation in November and March whole body energy density of juvenile Pacific herring in Prince William Sound, Alaska

Carbon Stable Isotope Analyses		
Model number	Response variable	Explanatory variables
1	Nov or Mar WBED (kJ/g)	~1, random = ~1 + FL|Collection Bay (null)
2	Nov or Mar WBED (kJ/g)	~FL + $\delta^{13}C'$, random = ~1 + FL|Collection Bay
3	Nov or Mar WBED (kJ/g)	~FL + Region, random = ~1 + FL|Collection Bay
4	Nov or Mar WBED (kJ/g)	~FL + Year, random = ~1 + FL|Collection Bay
5	Nov or Mar WBED (kJ/g)	~FL + $\delta^{13}C'$ + Region, random = ~1 + FL|Collection Bay
6	Nov or Mar WBED (kJ/g)	~FL + $\delta^{13}C'$ + Year, random = ~1 + FL|Collection Bay
7	Nov or Mar WBED (kJ/g)	~FL + Region + Year, random = ~1 + FL|Collection Bay
8	Nov or Mar WBED (kJ/g)	~FL + $\delta^{13}C'$ + Region + Year, random = ~1 + FL|Collection Bay
9	Nov or Mar WBED (kJ/g)	~FL + $\delta^{13}C'$ + Region + Year + $\delta^{13}C'$*Region, random = ~1 + FL|Collection Bay
10	Nov or Mar WBED (kJ/g)	~FL + $\delta^{13}C'$ + Region + Year + $\delta^{13}C'$*Year, random = ~1 + FL|Collection Bay
Nitrogen Stable Isotope Analyses		
Model number	Response variable	Explanatory variables
1	Nov or Mar WBED (kJ/g)	~1, random = ~1 + FL|Collection Bay (null)
2	Nov or Mar WBED (kJ/g)	~FL + $\delta^{15}N$, random = ~1 + FL|Collection Bay
3	Nov or Mar WBED (kJ/g)	~FL + Region, random = ~1 + FL|Collection Bay
4	Nov or Mar WBED (kJ/g)	~FL + Year, random = ~1 + FL|Collection Bay
5	Nov or Mar WBED (kJ/g)	~FL + $\delta^{15}N$ + Region, random = ~1 + FL|Collection Bay
6	Nov or Mar WBED (kJ/g)	~FL + $\delta^{15}N$ + Year, random = ~1 + FL|Collection Bay
7	Nov or Mar WBED (kJ/g)	~FL + Region + Year, random = ~1 + FL|Collection Bay
8	Nov or Mar WBED (kJ/g)	~FL + $\delta^{15}N$ + Region + Year, random = ~1 + FL|Collection Bay
9	Nov or Mar WBED (kJ/g)	~FL + $\delta^{15}N$ + Region + Year + $\delta^{15}N$*Region, random = ~1 + FL|Collection Bay

10	Nov or Mar WBED (kJ/g)	~FL + δ^{15}N + Region + Year + δ^{15}N*Year, random = ~1 + FL|Collection Bay

Abbreviations: WBED = whole body energy density, FL = fork length, $\delta^{13}C'$ = lipid corrected carbon stable isotope signature. $\delta^{15}N$ = nitrogen stable isotope signature.

Appendix B. Supporting information

Supplementary data associated with this article can be found in the online version at http://dx.doi.org/10.1016/j.dsr2.2017.10.010.

References

Beamer, J.P., Hill, D.F., Arendt, A., Liston, G.E., 2016. High-resolution modeling of coastal freshwater discharge and glacier mass balance in the Gulf of Alaska watershed. Water Resour. Res. 52, 3888–3909.

Blaxter, J.H., Holiday, F.G., 1963. The behavior and physiology of herring and other clupeids. Adv. Mar. Biol. 1, 261–393.

Bond, N.A., Cronin, M.F., Freeland, H., Mantua, N., 2015. Causes and impacts of the 2014 warm anomaly in the NE Pacific. Geophys. Res. Lett. 42, 3414–3420.

Brown, E.D., Norcross, B.L., Short, J.W., 1996. An introduction to studies on the effects of the Exxon Valdez oil spill on early life history stages of Pacific herring, *Clupea pallasi*, in Prince William Sound, Alaska. Can. J. Fish. Aquat. Sci. 53, 2337–2342.

Burnham, K.P., Anderson, D.R., 2002. Model Selection and Multi-Model Inference: A Practical Information Theoretic Approach. Springer-Verlag, New York, NY.

Cooney, R.T., 1986. The seasonal occurrence of *Neocalanus cristatus, Neocalanus plumchrus, and Eucalanus bungii* over the shelf of the northern Gulf of Alaska. Cont. Shelf Res. 5, 541–553.

Cooney, R.T., Allen, J.R., Bishop, M.A., Eslinger, D.L., Kline, T., Norcross, B.L., McRoy, C.P., Milton, J., Olsen, J., Patrick, V., Paul, A.J., Salmon, D., Scheel, D., Thomas, G.L., Vaughan, S.L., Willette, T.M., 2001a. Ecosystem control of pink salmon (*Oncorhynchus gorbuscha*) and Pacific herring (*Clupea pallasi*) populations in Prince William Sound, Alaska. Fish. Oceanogr. 10, 1–13.

Cooney, R.T., Coyle, K.O., Stockmar, E., Stark, C., 2001b. Seasonality in surface-layer net zooplankton communities in Prince William Sound, Alaska. Fish. Oceanogr. 10, 97–109.

Core Team, R., 2017. R: A Language and Environment for Statistical Computing. R Foundation for Statistical Computing, Vienna, Austria. ⟨https://www.r-project.org/⟩.

Coyle, K.O., Gibson, G.A., Hedstrom, K., Hermann, A.J., Hopcroft, R.R., 2013. Zooplankton biomass, advection and production on the northern Gulf of Alaska shelf from simulations and field observations. J. Mar. Syst. 128, 185–207.

Crawley, M.J., 2007. The R Book. John Wiley & Sons, Ltd, West Sussex, UK.

Damkaer, D.M., 1977. Initial Zooplankton Investigations in Prince William Sound, Gulf of Alaska, and lower Cook Inlet. Environmental Assessment of the Alaska Continental Shelf. Annual Reports of the Principal Investigators, for the Year Ending 1997 (Receptors – Fish, Littoral, Benthos). U.S. Dept. of Commerce, Washington D.C, pp. 137–274.

Deniro, M.J., Epstein, S., 1978. Influence of diet on distribution of carbon isotopes in animals. Geochim. Cosmochim. Acta 42, 495–506.

Deniro, M.J., Epstein, S., 1981. Influence of diet on the distribution of nitrogen isotopes in animals. Geochim. Cosmochim. Acta 45, 341–351.

Eslinger, D.L., Cooney, R.T., McRoy, C.P., Ward, A., Kline, T.C., Simpson, E.P., Wang, J., Allen, J.R., 2001. Plankton dynamics: observed and modelled responses to physical conditions in Prince William Sound, Alaska. Fish. Oceanogr. 10 (Suppl. 1), S81–S96.

Foy, R.J., Norcross, B.L., 1999. Feeding Behavior of Herring (*Clupea pallasi*) Associated with Zooplankton Availability in Prince William Sound, Alaska., Ecosystem Approaches for Fisheries Management (AK-SG-99-01). University of Alaska Sea Grant, Fairbanks, pp. 129–135.

Gorman, K.B., Kline Jr., T.C., Roberts, M.E., Sewall, F.S., Heintz, R.A., Pegau, W.S., 2017. Herring Condition Monitoring. Exxon Valdez Long-Term Herring Research and Monitoring Final Report (Restoration Project 16120111-L). Prince William Sound Science Center, Cordova, Alaska and NOAA Alaska Fisheries Science Center, Juneau, Alaska.

Halverson, M.J., Belanger, C., Gay, S.M., 2013a. Seasonal transport variations in the straits connecting Prince William Sound to the Gulf of Alaska. Cont. Shelf Res. 63, S63–S78.

Halverson, M.J., Ohlmann, J.C., Johnson, M.A., Pegau, W.S., 2013b. Disruption of a cyclonic eddy circulation by wind stress in Prince William Sound, Alaska. Cont. Shelf Res. 63, S13–S25.

Johnson, W.R., Royer, T.C., Luick, J.L., 1988. On the seasonal variability of the Alaska Coastal Current. J. Geophys. Res. Oceans 93, 12423–12437.

Kelly, J.F., 2000. Stable isotopes of carbon and nitrogen in the study of avian and mammalian trophic ecology. Can. J. Zool. 78, 1–27.

Kline, T.C., 1997. Confirming forage fish food web dependencies in Prince William Sound using natural stable isotope tracers, Forage Fishes in Marine Ecosystems. In: Proceedings of the International Symposium on the Role of Forage Fishes in Marine Ecosystems. University of Alaska Sea Grant College Program, pp. 257–269.

Kline, T.C., 1999a. Monitoring Changes in Oceanographic Forcing using the Carbon and Nitrogen Isotopic Composition of Prince William Sound pelagic biota, Ecosystem Approaches for Fisheries Management (AK-SG-99-01). University of Alaska Sea Grant, Fairbanks, pp. 87–95.

Kline, T.C., 1999b. Temporal and spatial variability of C-13/C-12 and N-15/N-14 in pelagic biota of Prince William Sound, Alaska. Can. J. Fish. Aquat. Sci. 56, 94–117.

Kline, T.C., 2009. Characterization of carbon and nitrogen stable isotope gradients in the northern Gulf of Alaska using terminal feed stage copepodite-V *Neocalanus cristatus*. Deep-Sea Res. II 56, 2537–2552.

Kline, T.C., 2013. PWS Herring Survey: Pacific Herring Energetic Recruitment Factors. Exxon Valdez Oil Spill Restoration Project Final Report (Project 10100132-C).

Kline, T.C., Campbell, R.W., 2010. Prince William Sound Herring Forage Contingency. Exxon Valdez Oil Spill Restoration Project Final Report (Project 070811).

Kline, T.C., 2000. Trophic position of Pacific herring in Prince William Sound, Alaska, based on their stable isotope abundance, In: Funk, F., Blackburn, J., Hay, D., Paul, A. J., Stephenson, R., Toresen, R., Witherell, D. (Eds.), Herring: Expectations for a New Millennium, pp. 69–80.

Kline, T.C., 2001. Evidence of biophysical coupling from shifts in abundance of natural stable carbon and nitrogen isotopes in Prince William Sound, Alaska, In: Kruse, G.H., Bez, N., Booth, A., Dorn, M.W., Hills, S., Lipcius, R.N., Pelletier, D., Roy, C., Smith, S. J., Witherell, D. (Eds.), Spatial Processes and Management of Marine Populations, pp. 363–376.

Mazerolle, M.J., 2017. AICcmodavg: model selection and multimodel inference based on (Q)AIC(c). R. Package Version 2 (1-1). ⟨https://cran.r-project.org/package=AICcmodavg⟩.

McConnaughey, T., McRoy, C.P., 1979. Food-web structure and the fractionation of carbon isotopes in the Bering Sea. Mar. Biol. 53, 257–262.

Muradian, M.L., Branch, T.A., Moffitt, S.D., Hulson, P.J.F., 2017. Bayesian stock assessment of Pacific herring in Prince William Sound, Alaska. PLoS ONE 12, 29.

Musgrave, D.L., Halverson, M.J., Pegau, W.S., 2013. Seasonal surface circulation, temperature, and salinity in Prince William Sound, Alaska. Cont. Shelf Res. 53, 20–29.

Niebauer, H.J., Royer, T.C., Weingartner, T.J., 1994. Circulation of Prince William Sound, Alaska. J. Geophys. Res. Oceans 99, 14113–14126.

Norcross, B.L., Brown, E.D., Foy, R.J., Frandsen, M., Gay, S.M., Kline, T.C., Mason, D.M., Patrick, E.V., Paul, A.J., Stokesbury, K.D.E., 2001. A synthesis of the life history and ecology of juvenile Pacific herring in Prince William Sound, Alaska. Fish. Oceanogr. 10, 42–57.

Parr Instrument Company, 2009. Introduction to Bomb Calorimetry, Moline, Illinois.

Paul, A.J., Paul, J.M., 1998. Comparisons of whole body energy content of captive fasting age zero Alaskan Pacific herring (*Clupea pallasi Valenciennes*) and cohorts over-wintering in nature. J. Exp. Mar. Biol. Ecol. 226, 75–86.

Paul, A.J., Paul, J.M., 1999. Interannual and regional variations in body length, weight and energy content of age-0 Pacific herring from Prince William Sound, Alaska. J. Fish. Biol. 54, 996–1001.

Paul, A.J., Paul, J.M., Brown, E.D., 1998. Fall and spring somatic energy content for Alaskan Pacific herring (Clupea pallasi Valenciennes 1847) relative to age, size and sex. J. Exp. Mar. Biol. Ecol. 223, 133–142.

Paul, A.J., Paul, J.M., Kline Jr., T.C., 2001. Estimating whole body energy content for juvenile Pacific herring from condition factor, dry weight, and carbon/nitrogen ratio (AK-SG-01-04) In: Funk, F., Blackburn, J., Hay, D., Paul, A.J., Stephenson, R., Toresen, R., Witherell, D. (Eds.), Herring: Expectations for a New Millennium. University of Alaska Sea Grant, Fairbanks, pp. 121–133.

Peterson, B.J., Fry, B., 1987. Stable isotopes in ecosystem studies. Annu. Rev. Ecol. Syst. 18, 293–320.

Pinheiro, J., Bates, D., DebRoy, S., Sarkar, D., Core Team, R., 2017. nlme: linear and nonlinear mixed effects models. R. Package Version 3, 1–131. ⟨https://cran.r-project.org/package=nlme⟩.

Royer, T.C., 1979. Effect of precipitation and runoff on coastal circulation in the Gulf of Alaska. J. Phys. Oceanogr. 9, 555–563.

Stabeno, P.J., Reed, R.K., 1991. Recent Lagrangian measurements along the Alaskan Stream. Deep-Sea Res. 38, 289–296.

Vaughan, S.L., Mooers, C.N.K., Gay, S.M., 2001. Physical variability in Prince William Sound during the SEA study (1994-98). Fish. Oceanogr. 10, 58–80.

Walther, B.D., Thorrold, S.R., Olney, J.E., 2008. Geochemical signatures in otoliths record natal origins of American shad. T. Am. Fish. Soc. 137, 57–69.

Wang, J., Jin, M.B., Patrick, E.V., Allen, J.R., Eslinger, D.L., Mooers, C.N.K., Cooney, R.T., 2001. Numerical simulations of the seasonal circulation patterns and thermohaline structures of Prince William Sound, Alaska. Fish. Oceanogr. 10, 132–148.

Ward, E.J., Adkison, M., Couture, J., Dressel, S.C., Litzow, M.A., Moffitt, S., Neher, T.H., Trochta, J., Brenner, R., 2017. Evaluating signals of oil spill impacts, climate, and species interactions in Pacific herring and Pacific salmon populations in Prince William Sound and Copper River, Alaska. PLoS ONE 12, e0172898.

Weingartner, T.J., Danielson, S.L., Royer, T.C., 2005. Freshwater variability and predictability in the Alaska Coastal Current. Deep-Sea Res. II 52, 169–191.

Xu, R., 2003. Measuring explained variation in linear mixed effects models. Stat. Med. 22, 3527–3541.